

Holographic Wigner distributions for the pion

Mohammad Ahmady^{a,*}, Chandan Mondal^{b,†}, Ruben Sandapen^{c,‡},
James P. Vary^{d,§} and Xingbo Zhao^{a,e,||}

^aMount Allison University, Sackville, New Brunswick, Canada, E4L 1E6

^bInstitute of Modern Physics, Chinese Academy of Sciences, Lanzhou-730000, China

^cAcadia University, Wolfville, Nova-Scotia, Canada, B4P 2R6

^dIowa State University, Ames, IA 50011, USA

^eSchool of Nuclear Science and Technology, University of Chinese Academy of Sciences, Beijing 100049, China

*mahmady@mta.ca

†mondal@impcas.ac.cn

‡ruben.sandapen@acadiau.ca

§jvary@iastate.edu

||xbzhao@impcas.ac.cn

We study the Wigner distributions of the pion using a holographic light-front pion wavefunction with dynamical spin effects to reveal its multidimensional structure.

Keywords: Wigner distributions; Light-front holography; Light mesons.

1. Introduction

Wigner distributions in QCD, commonly known as phase-space distributions, were first introduced by Ji¹. After appropriate phase-space reductions, these distributions reduce to generalized parton distributions (GPDs) and transverse momentum dependent parton distributions (TMDs) which are measurable in high energy experiments (For a review on these distributions and the experiments to measure them, see²⁻⁵). GPDs allow us to have a three dimensional picture of the hadron in position space⁶. On the other side, TMDs contains three dimensional information regarding the spin-spin and spin-orbit correlations in momentum space⁷. Wigner distributions for spin- $\frac{1}{2}$ systems have been investigated in different models e.g., light-cone chiral quark soliton model⁸, light-front dressed quark model⁹, light-cone spectator model¹⁰, AdS/QCD inspired quark-diquark model^{11,12} as well as light front QED model¹³.

Here, we study the Wigner distributions for different quark polarizations in the pion using a holographic light-front pion wavefunction which

includes dynamical spin effects. It has been observed that such effects allow for an excellent simultaneous description of a wide range of data: the decay constant, charge radius, spacelike EM and transition form factors, as well as, after QCD evolution, both the parton distribution function and the parton distribution amplitude data with a single universal AdS/QCD scale¹⁴. Recently, this spin-improved holographic wavefunction has been used to predict the leading twist TMDs of the pion¹⁵.

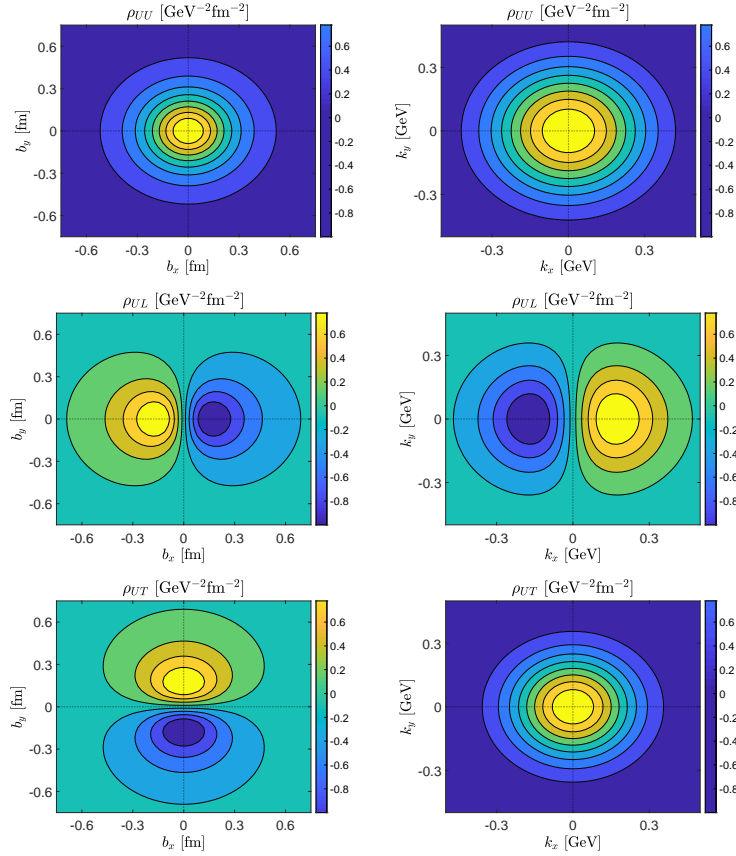


Fig. 1. Wigner distribution $\rho(\mathbf{b}_\perp, \mathbf{k}_\perp)$ of the unpolarized quark (*upper panels*), the longitudinal polarized quark (*middle panels*), and the transversely polarized quark (*lower panels*) inside the pion. (*Left panels*) the distributions are in the impact-parameter space with fixed transverse momentum $\mathbf{k}_\perp = k_\perp \hat{e}_y$ and $k_\perp = 0.3$ GeV. (*Right panels*) the distributions are in the transverse-momentum space with fixed impact parameter $\mathbf{b}_\perp = b_\perp \hat{e}_y$ and $b_\perp = 0.3$ fm.

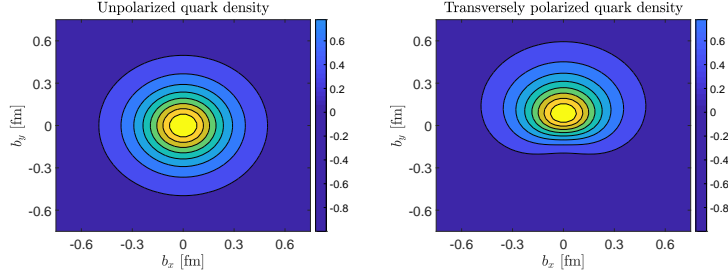


Fig. 2. Transverse spin densities of pion for unpolarized quark (left panel) and transversely polarized (along \hat{x}) quark (right panel).

2. Wigner distributions

Wigner distributions are defined as⁸

$$\rho^{[\Gamma]}(x, \mathbf{b}_\perp, \mathbf{k}_\perp) = \int \frac{d^2 \Delta_\perp}{(2\pi)^2} e^{-i\Delta_\perp \cdot \mathbf{b}_\perp} W^{[\Gamma]}(x, \Delta_\perp, \mathbf{k}_\perp), \quad (1)$$

where $W^{[\Gamma]}(x, \Delta_\perp, \mathbf{k}_\perp)$ is the generalized correlator at $\xi = \Delta^+/P^+ = 0$, and \mathbf{b}_\perp is the impact parameter in the position space conjugate to Δ_\perp . Explicitly,

$$W^{[\Gamma]} = \int \frac{dz^- d^2 \mathbf{z}_\perp}{2(2\pi)^3} e^{ik \cdot z} \langle p' | \bar{\psi}(-\frac{1}{2}z) \Gamma \mathcal{W} \psi(\frac{1}{2}z) | p \rangle \Big|_{z^+=0}, \quad (2)$$

with $\Gamma \equiv \{\gamma^+, \gamma^+ \gamma^5, i\sigma^{j+} \gamma_5\}$. We define the initial and final momenta of the pion in a symmetric frame as $p' = (p^+, p'^-, \frac{\Delta_\perp}{2})$ and $p'' = (p^+, p''^-, -\frac{\Delta_\perp}{2})$, respectively. For instance,

$$\begin{aligned} W^{[\gamma^+]}(x, \Delta_\perp, \mathbf{k}_\perp) &= \sum_{h', h, \bar{h}} \Psi_{h'\bar{h}}^*(x, \mathbf{k}_\perp'') \chi_{h'}^\dagger \chi_h \Psi_{h\bar{h}}(x, \mathbf{k}_\perp'), \\ W^{[\gamma^+ \gamma_5]}(x, \Delta_\perp, \mathbf{k}_\perp) &= \sum_{h', h, \bar{h}} \Psi_{h'\bar{h}}^*(x, \mathbf{k}_\perp'') \chi_{h'}^\dagger \sigma_3 \chi_h \Psi_{h\bar{h}}(x, \mathbf{k}_\perp'), \\ W^{[i\sigma^{j+} \gamma_5]}(x, \Delta_\perp, \mathbf{k}_\perp) &= \sum_{h', h, \bar{h}} \Psi_{h'\bar{h}}^*(x, \mathbf{k}_\perp'') \chi_{h'}^\dagger \sigma_j \chi_h \Psi_{h\bar{h}}(x, \mathbf{k}_\perp'), \end{aligned}$$

where σ_i are the Pauli spin matrices and χ_h is the helicity spinor. The arguments \mathbf{k}_\perp' and \mathbf{k}_\perp'' of the light-front wavefunctions are given by $\mathbf{k}_\perp' = \mathbf{k}_\perp - (1-x)\frac{\Delta_\perp}{2}$, and $\mathbf{k}_\perp'' = \mathbf{k}_\perp + (1-x)\frac{\Delta_\perp}{2}$. One then can classify the

unpolarized, longitudinally polarized and transversely polarized Wigner distributions in pion as: $\rho_{UU}(x, \mathbf{b}_\perp, \mathbf{k}_\perp) = \rho^{[\gamma^+]}(x, \mathbf{b}_\perp, \mathbf{k}_\perp)$, $\rho_{UL}(x, \mathbf{b}_\perp, \mathbf{k}_\perp) = \rho^{[\gamma^+\gamma_5]}(x, \mathbf{b}_\perp, \mathbf{k}_\perp)$, and $\rho_{UT}(x, \mathbf{b}_\perp, \mathbf{k}_\perp) = \rho^{[i\sigma^{j+}\gamma_5]}(x, \mathbf{b}_\perp, \mathbf{k}_\perp)$, respectively.

We compute the pion Wigner distributions using the spin-improved holographic light-front wavefunctions given by¹⁴

$$\Psi_{h,\bar{h}}(x, \mathbf{k}) = [(M_\pi x\bar{x} + Bm_f)h\delta_{h,-\bar{h}} - Bk_\perp e^{-ih\theta_{k_\perp}}\delta_{h,\bar{h}}] \frac{\Psi(x, k_\perp^2)}{x\bar{x}}. \quad (3)$$

We refer to B as the dynamical spin parameter. $B \rightarrow 0$ means no spin-orbit correlations as in the original holographic wavefunction¹⁶, while $B \geq 1$ corresponds to a maximal spin-orbit correlations. With $B \geq 1$, $m_{u/d} = 330$ MeV and a universal AdS/QCD scale, $\kappa = 523$ MeV, we successfully predict simultaneously the pion decay constant, charge radius, spacelike electromagnetic and transition form factors, the pion parton distribution functions after taking into account perturbative QCD evolution.

3. Results

In Fig. 1, we show the first Mellin moments of Wigner distributions ρ_{UU} , ρ_{UL} and ρ_{UT} for the pion in the upper, central and lower panels. The left panels plot the distributions in the impact-parameter space with fixed transverse momentum $\mathbf{k}_\perp = k_\perp \hat{e}_y$ and $k_\perp = 0.3$ GeV, while the right panels plot the distributions in the transverse-momentum space with fixed impact parameter $\mathbf{b}_\perp = b_\perp \hat{e}_y$ and $b_\perp = 0.3$ fm. We find no distortions in unpolarized quark distributions in both the transverse momentum space and the impact parameter space. They both are circularly symmetric. However, we observe the dipolar distortion patterns for the longitudinally polarized quark in both spaces and for the transversely polarized quark in impact parameter space only. For the longitudinally polarized quark, the polarity of the impact space distribution is opposite to that in momentum space. When the quark is transversely polarized along x -direction, the deformation in b_\perp space appears in y -direction. These deformation patterns are similar to those of the valence quark distributions of the proton considered as a quark-diquark system¹¹.

Lattice QCD calculations give access to x moments of quark spin densities. To compare with lattice results, we compute the spin density for the transversely polarized quark:

$$\rho_T(\mathbf{b}_\perp) = \frac{1}{2} \int dx d^2\mathbf{k}_\perp x [\rho_{UU}(x, \mathbf{b}_\perp, \mathbf{k}_\perp) + s_T \rho_{UT}(x, \mathbf{b}_\perp, \mathbf{k}_\perp)]. \quad (4)$$

Fig. 2 shows that the unpolarized density is axially symmetric with the peak at the center of pion ($b_{\perp} = 0$), while due to the dipolar distortion from ρ_{UT} , the resulting distribution for a transversely polarized (along +ve \hat{x}) quark gets shifted toward positive \hat{y} . Our predictions for spin distributions are in qualitative agreement with lattice results¹⁷.

Acknowledgements: MA and RS are supported by NSERC (Canada) Grants: SAPIN-2017-00033 and SAPIN-2017-00031, respectively. CM is supported by NSFC (China) under the Grant Nos. 11850410436 and 11950410753. JPV is supported by the DoE under Grants No. DE-FG02-87ER40371, and No. DE-SC0018223 (SciDAC4/NUCLEI). XZ is supported by new faculty startup funding by IMPCAS by Key Research Program of Frontier Sciences, CAS Grant No. ZDBS-LY-7020.

References

1. X. Ji, Phys. Rev. Lett. **91** 062001 (2003).
2. X. Ji, J. Phys. G **24** 1181 (1998).
3. K. Goeke *et al.*, Prog. Part. Nucl. Phys. **47** 401 (2001).
4. P. Mulders and R. Tangerman, Nucl. Phys. B **461**, 197 (1996).
5. D. Boer and P. J. Mulders, Phys. Rev. D **57**, 5780 (1998).
6. M. Burkardt, Int. J. Mod. Phys. A **18**, 173 (2003).
7. C. Lorcé and B. Pasquini, Phys. Rev. D **84**, 034039 (2011).
8. C. Lorcé and B. Pasquini, Phys. Rev. D **84**, 014015 (2011).
9. A. Mukherjee *et al.*, Phys. Rev. D **90**, 014024 (2014).
10. T. Liu and B.-Q. Ma, Phys. Rev. D **91**, 034019 (2015).
11. D. Chakrabarti, T. Maji, C. Mondal and A. Mukherjee, Eur. Phys. J. C **76**, no. 7, 409 (2016).
12. D. Chakrabarti, T. Maji, C. Mondal and A. Mukherjee, Phys. Rev. D **95**, no. 7, 074028 (2017).
13. N. Kumar and C. Mondal, Nucl. Phys. B **931**, 226 (2018).
14. M. Ahmady, C. Mondal and R. Sandapen, Phys. Rev. D **98**, 034010 (2018).
15. M. Ahmady, C. Mondal and R. Sandapen, Phys. Rev. D **100**, no. 5, 054005 (2019).
16. S. J. Brodsky *et al.*, Phys. Rept. **584**, 1 (2015).
17. D. Brommel *et al.*, Phys. Rev. Lett. **101**, 122001 (2008).